

Electrical Resistivity of Polycarbonate/Multiwalled Carbon Nanotube Composites Under Varying Injection Molding Conditions

Dong Hyun Park,¹ Kwan Han Yoon,¹ Young-Bin Park,² Young Sil Lee,³ Young Jun Lee,³ Sang Wan Kim³

¹Department of Polymer Science and Engineering, Kumoh National Institute of Technology, Gumi, Gyeongbuk 730-701, Korea

²Department of Industrial and Manufacturing Engineering, FAMU-FSU College of Engineering, Tallahassee, Florida 32310-6046

³Samsung Cheil Industries Inc., 332-2 Gocheon-dong, Uiwang-Si, Gyeonggi-do 437-711, Korea

Received 18 September 2007; accepted 1 January 2009

DOI 10.1002/app.29989

Published online 19 March 2009 in Wiley InterScience (www.interscience.wiley.com).

ABSTRACT: Multiwalled carbon nanotube (MWCNT)-filled polycarbonate composites were prepared by a corotating intermeshing twin-screw extruder. The surface resistivities of compression- and injection-molded specimens were quite different, the difference ranging from 10^3 to 10^7 Ω/sq at varying MWCNT concentrations. The surface resistivity of the injection-molded specimen at 2 wt % loading varied up to 10^5 Ω/sq in the specimen thickness direction and up to 10^4 Ω/sq in the polymer flow direction with respect to the gate. The difference in surface resistivity with the positions of injection-molded specimen was confirmed with the morphology, which showed the differ-

ence in MWCNT number density (numbers/surface area). There was no significant effect on surface resistivity with injection pressure, holding pressure, and molding temperature. The specimens prepared at the injection speed of 13 mm/s showed surface resistivities 10^3 – 10^4 Ω/sq depending on the positions, which was comparable with the compression-molded specimens, which had a surface resistivity of 10^3 Ω/sq . © 2009 Wiley Periodicals, Inc. *J Appl Polym Sci* 113: 450–455, 2009

Key words: polycarbonate; nanocomposites; morphology; electrical resistivity; injection molding

INTRODUCTION

Carbon nanotubes (CNTs) are very effective filler in polymeric matrices when one desires enhanced mechanical properties^{1–5} and conductive materials^{6–9} because of their electrical conductivity at very low loadings. A key issue in producing a polymer/CNT composite application is how to achieve a homogeneous dispersion of CNTs in the polymeric matrices. Currently, three methods commonly are used to incorporate CNTs into polymers: (i) solution processing, (ii) in situ polymerization of the CNT-polymer monomer mixture, and (iii) melt mixing of CNTs with polymers. In context with industrial applications, melt mixing is the preferred method of composite preparation because of its scalability. The tendency of CNTs to form aggregates may be minimized by the appropriate application of shear during melt mixing.⁸ Here, two ways of introducing CNTs in polymer matrices are used: (i) CNTs can be directly added to polymers during melt mixing or

(ii) commercially available masterbatches of CNT/polymer composites can be used as a starting material and diluted by adding an appropriate amount of pure polymer in a subsequent melt mixing process.

Recently, the electrical resistivities of polycarbonate (PC)/multiwalled carbon nanotube (MWCNT) composites were investigated by the dilution method using masterbatch. Chen et al.¹⁰ reported that the electrical resistivity measurements of the PC/MWCNT composite indicated a percolation of MWCNT near 5 wt % for the composites. Satapathy et al.¹¹ have shown that the composite with only 2 wt % MWCNT is already conductive. In their work, the electrical resistivity of the composites was measured on strips cut from compression molding sheets. In our preliminary test, we found that the electrical resistivity of PC/MWCNT composite decreased considerably after injection molding compared with compression molding specimen. The difference in electrical resistivity values between compression molded and injection molded specimens ranged between 10^3 and 10^7 Ω/sq , depending on MWCNT loading.

In this work, we tried to reduce the difference in electrical resistivity value between compression-molded and injection-molded specimens by

Correspondence to: K. H. Yoon (khyoon@kumoh.ac.kr).

controlling the injection molding conditions. The densities of MWCNT at various locations of injection molded specimens were observed by scanning electron microscopy (SEM).

EXPERIMENTAL

Materials

The MWCNTs used in this study were manufactured by the chemical vapor deposition (CVD) process and supplied from Hanwha/Nanotech (Incheon, Korea) (purity >97%, length: 10–50 μm , diameter: 10–20 nm, surface resistivity $<10^{-4}$ Ω/sq). PC, granule type was obtained from Samsung Cheil Industries Inc. (Uiwang-Si, Korea), and its weight average molecular weight, M_w and surface resistivity were 22,000 g/mol and 10^{16} Ω/sq , respectively.

Preparation of PC/MWCNT composites

Before the preparation of PC/MWCNT composites, PC was mixed with MWCNT at different loading by ball-milling with mixed ball sizes of 1.0 and 2.0 mm for 6 h to improve the dispersion of MWCNT into PC matrix. Then, the PC/MWCNT composites containing 1, 2, 3, and 5 wt % MWCNTs were produced in a corotating intermeshing twin-screw extruder ($D = 30$ mm, $L/D = 42$) in kilogram scale. The barrel temperatures from the entrance to the exit were 200, 250, 260, 270, 270, and 270°C, respectively. The composite pellets obtained were compression molded into $80 \times 40 \times 3$ mm³ specimens by use of a hot press for 2 min at 270°C under 138 MPa. Injection molding was conducted with the use of LSIDE75EN Injection molding (75 ton) of which the screw diameter, maximum injection pressure, maximum injection speed, cooling time, and barrel temperature are 32 mm, 178 MPa, 63 mm/s, 15 s, and 300°C, respectively. The size of injection molded specimen was identical with the compression molded one.

Characterizations

Morphology of PC/MWCNT composites was examined by scanning electron microscopy (SEM, S-4300, Hitachi). The surface resistivity of PC/MWCNT composites was measured by electrometers (R8340A, ADVANTEST, JP). The samples were measured by the four-probe method, and an average of four tests per specimen was used.

RESULTS AND DISCUSSION

To examine the state of percolation in PC/MWCNT composites, surface resistivity was measured. Figure 1 shows the surface resistivities of compression-

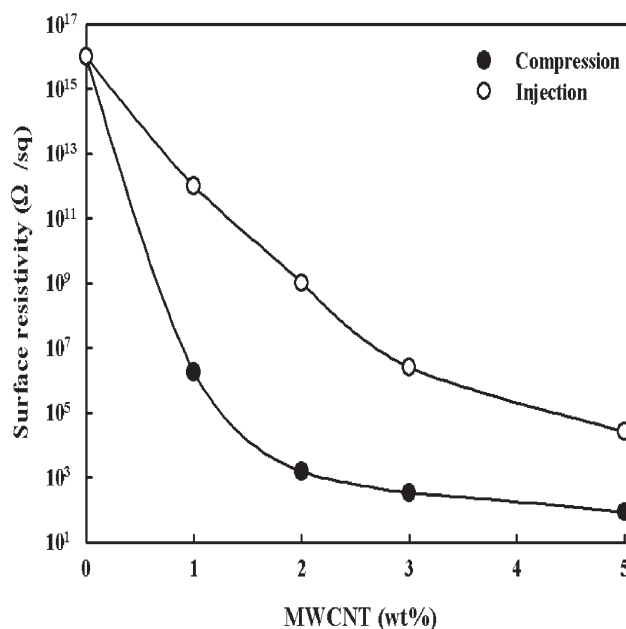


Figure 1 Surface resistivity of compression-molded and injection-molded specimens for PC/MWCNT composite as a function of the MWCNT concentration.

molded and injection-molded specimens as a function of the MWCNT concentration. For compression-molded specimens, the surface resistivity decreases with increasing nanotube concentration. Near 2 wt % the surface resistivity changed greatly. At concentrations greater than 2 wt % MWCNT, the surface resistivities were low and decreased marginally with the increasing MWCNT concentration. This result indicates that the great decrease in surface resistivity of the composite should, presumably, result from the formation of the conductive network structure. The composite containing greater than 2 wt % can be regarded as electrically conductive. This percolation threshold is in accordance with the results reported in the literature.^{10,12–16}

For injection-molded specimens, quite different results were observed. The surface resistivities of injection-molded specimens were greater than those of compression molded specimens at the same MWCNT loadings, the difference ranging between 10^3 and 10^7 Ω/sq . The increase in resistivity for injection-molded specimen may result from the orientation and alignment of MWCNTs. Recently, Pötschke et al.¹⁵ reported that PC/MWCNT composite at 2 wt % loading showed a volume resistivity of 550 Ω cm, whereas pure PC showed the value in the range of 10^{17} Ω cm. However, the fibers and their bundles were not conductive anymore because of the nanotube orientation and alignment. This finding was in accordance with investigations made by Hagenmueller et al.⁸ on melt-processed SWNT/PMMA films, which showed high electrical conductivity at

low draw ratios but conductivities below the detection limit at draw ratios much greater than four. However, the increase in resistivity for injection-molded specimens may not result from the orientation and alignment of MWCNTs.

Figure 2 shows the morphology of two different specimens at 2 wt % MWCNT loading. It was difficult to see MWCNTs from the surface of the composite specimen because the surface was covered with PC. Therefore, the morphologies in Figure 2 were observed on the surface stripped in the surface direction of the specimen. It is shown that there is a significant difference in number density (numbers/surface area) of MWCNT between two specimens. The number density of MWCNT in the compression-molded specimen was greater than that of injection-molded one. It is thought that low number density in the injection-molded specimen results from the different flowability between MWCNT and PC during injection molding. To investigate this phenomenon further, the surface resistivity in the direction of depth of the injection-molded specimen was measured and presented in Figure 3. It was observed that there is a large difference of $10^5 \Omega/\text{sq}$ in surface resistivity from the surface to center of specimen. Therefore, we tried to control the surface

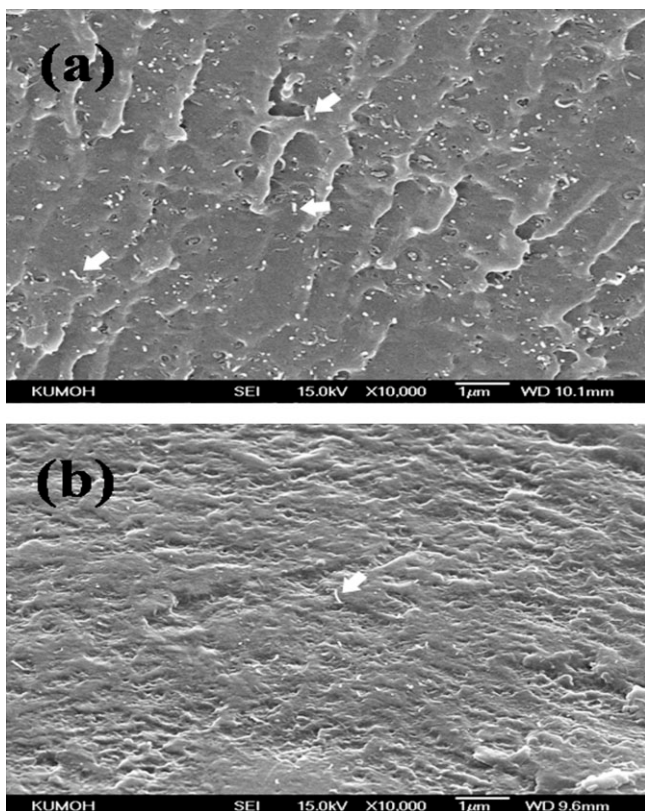


Figure 2 SEM images of (a) compression-molded and (b) injection-molded specimen for PC/MWCNT composites at 2 wt % loading.

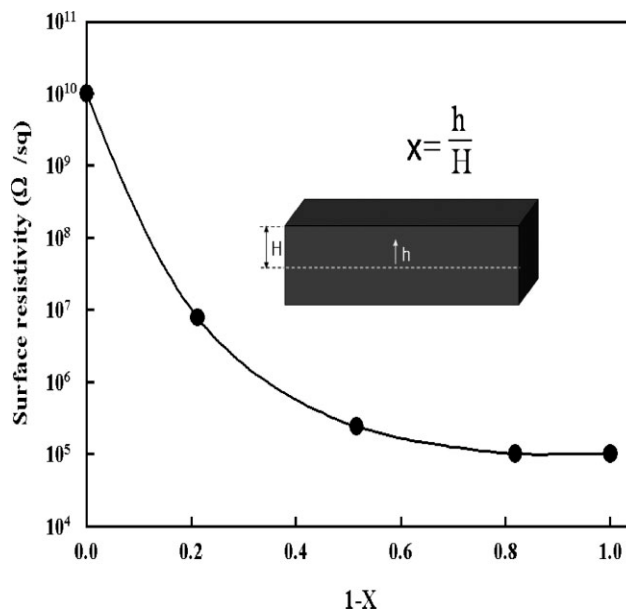


Figure 3 Surface resistivity in the direction of depth from surface of injection-molded specimen for PC/MWCNT composites at 2 wt % loading.

resistivity of injection-molded specimen to have the similar surface resistivity of compression molded specimen at 2 wt % loading by controlling injection molding conditions.

Figure 4 shows the surface resistivities of the injection-molded specimens at 2 wt % loading under various injection molding conditions. The surface resistivity of specimen was measured at three different regions with respect to the gate-top, middle, and end. Figure 4(a) shows the variation of surface resistivity with injection pressure (36, 53, 71, and 114 MPa). Holding pressure, mold temperature, and injection speed were 83 MPa, 60°C , and 22 mm/s, respectively. The surface resistivities for the “end” region of specimen were almost constant with injection pressure and were greater than $10^{10} \Omega/\text{sq}$. However, the surface resistivities for “top” and “middle” regions decreased considerably at 53 MPa and leveled off thereafter. It indicates that the nanotubes do not flow to the end of specimen from the gate (i.e. specimen is resin-rich in the “end” region) under these operating conditions. The surface resistivities of injection molded specimens with injection pressure still showed higher values than compression molded specimens at the same nanotube loading. The injection pressure is fixed at 114 MPa in subsequent injection molding experiments.

Figure 4(b) shows the variation of surface resistivity with holding pressure (36, 53, 71, and 83 MPa). The other conditions were identical to Figure 4(a). The differences in surface resistivities for “top” and “middle” regions were not observed, whereas the surface resistivities for the “end” region showed

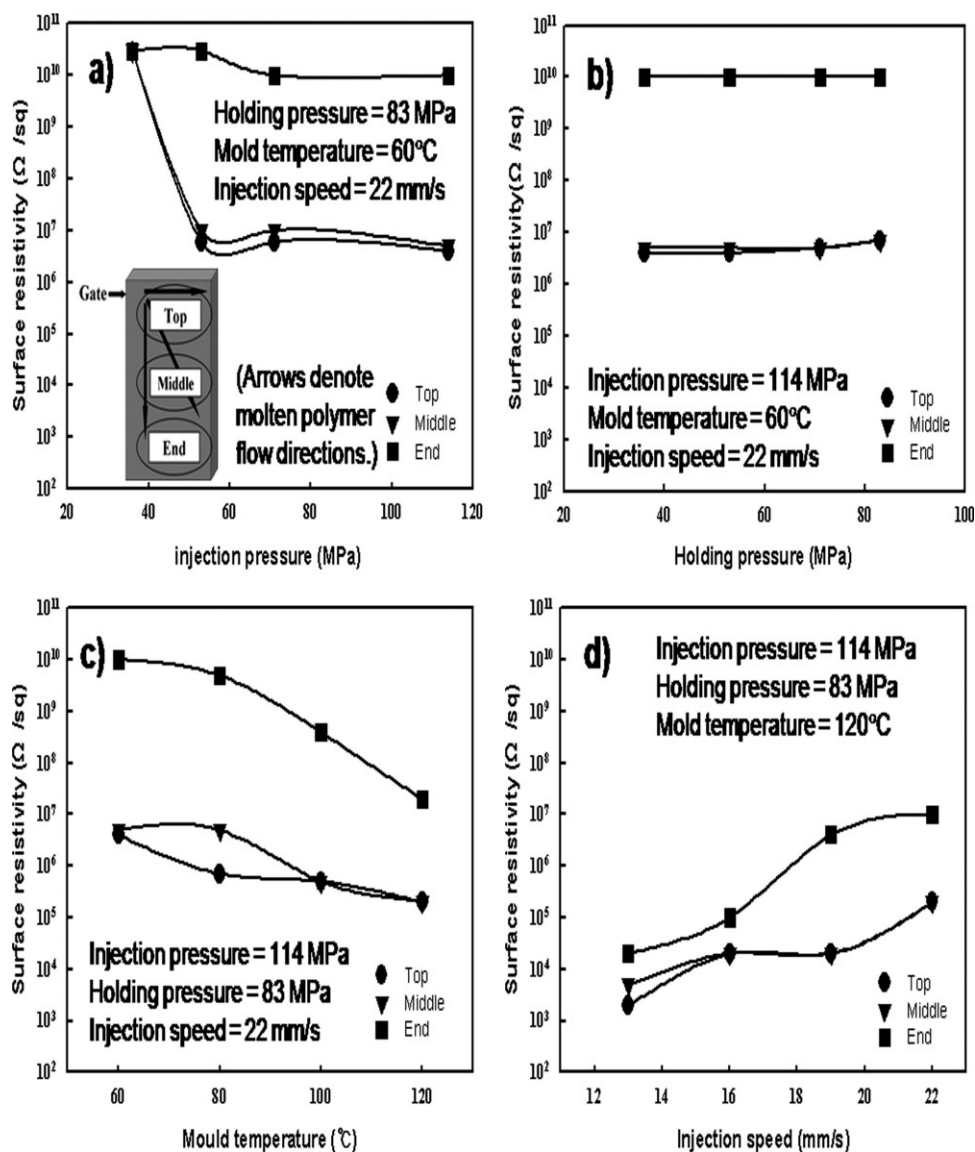


Figure 4 Surface resistivity for the positions of injection molded specimen with (a) injection pressure, (b) holding pressure, (c) molding temperature, and (d) injection speed, respectively.

large differences compared with the other two regions. Until now, the surface resistivity with injection pressure and holding pressure were investigated. These operating conditions do not affect the surface resistivity of the injection-molded specimen. The large difference in surface resistivity with the positions with respect to the gate was observed. Figure 5 shows the morphologies of “top” and “end” regions of specimens prepared at holding pressure of 83 MPa. There is a large difference in nanotube density between these two regions, resulting in the difference for surface resistivity. Holding pressure was fixed at 83 MPa in subsequent experiments.

Figure 4(c) shows the variation of surface resistivity with molding temperature. The fixed values of 114 and 83 MPa as aforementioned were used as

injection and holding pressure, respectively, and injection speed was 22 mm/s. The surface resistivity of three regions decreased with increasing mold temperature. In particular, the decreasing trend was evident in the “end” region. This finding suggests that molding temperature plays an important role in facilitating the nanotubes flow into the “end” of specimen from gate. The molding temperature was fixed at 120°C in subsequent experiments.

Figure 4(d) shows the variation of surface resistivity with injection speed (13, 16, 19, and 22 mm/s). The other conditions were as mentioned previously. Generally, the melt speed of polymer is dependent on the injection speed. However, the surface resistivity increases with increasing injection speed. It arises from the difference in flowability between nanotubes

and PC melt. The PC melt flows more quickly as compared with the nanotube. If the injection speed is low, the difference in flowability between nanotubes and PC melt decreases relatively. This result is well observed at low injection speed in Figure 4(d), in which the surface resistivity of the “end” region is close to those of “middle” and “top” regions. The surface resistivity values of the specimen made at injection speed of 13 mm/s are below $10^5 \Omega/\text{sq}$. Figure 6 shows the nanotube densities between “top” and “end” regions of specimen made under this operating condition. No notable difference in nanotube density was observed.

CONCLUSIONS

In this study, PC/MWCNT composites were prepared through a traditional industry scale plastic-processing method. The surface resistivities of compression-molded and injection-molded specimens were measured. The surface resistivities of two types of specimens were quite different, the difference ranging between 10^3 and $10^7 \Omega/\text{sq}$, depending on nanotube loading. To reduce the difference in surface resistivity between the two types of specimens,

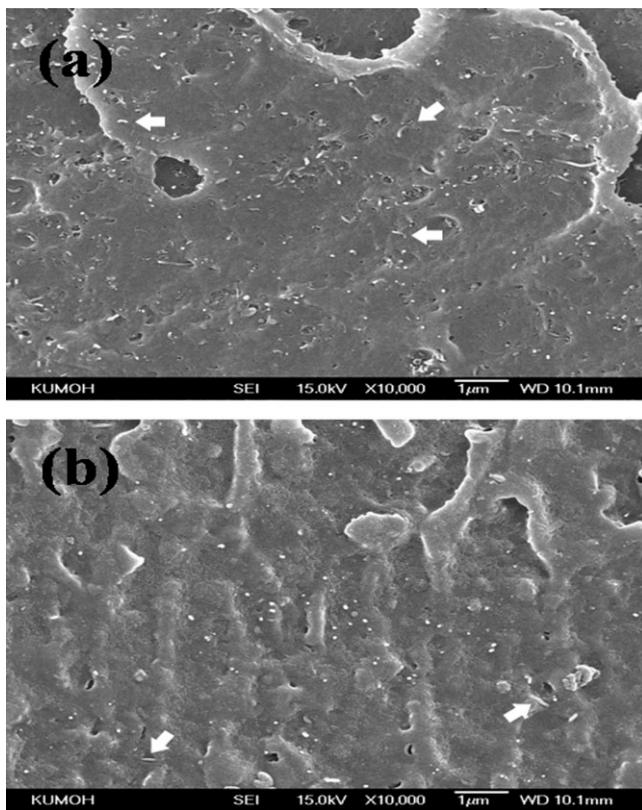


Figure 5 SEM images of (a) top and (b) end regions of injection molded specimen prepared at injection pressure of 114 MPa, holding pressure of 83 MPa, molding temperature of 60°C, and injection speed of 22 mm/s, respectively.

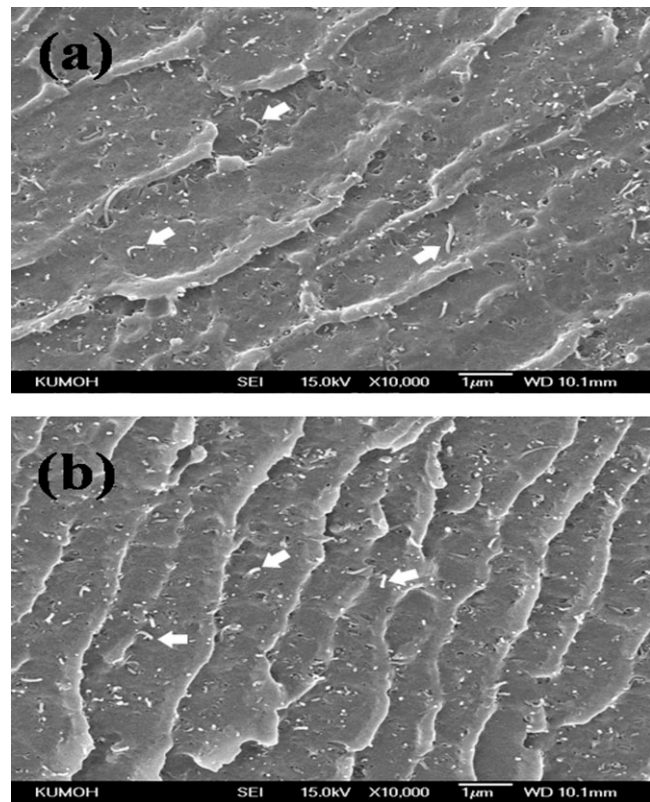


Figure 6 SEM images of (a) top and (b) end regions of injection molded specimen prepared with optimum operating conditions. (injection pressure of 114 MPa, holding pressure of 83 MPa, molding temperature of 120°C, and injection speed of 13 mm/s, respectively).

injection molding was performed under various operating conditions. Because of the nature of injection molding process, which induces nonuniform distribution of nanofillers as the result of the flowability difference between polymer and fillers, the surface resistivity difference were observed at various positions with respect to the gate. There were no significant effects of injection pressure, holding pressure, and molding temperature on surface resistivity. However, the injection speed played an important role in reducing the difference in surface resistivity with the positions of injection molded specimen, resulting in reduced difference in surface resistivity between compression and injection molded specimens. The optimization of injection molding conditions that allows consistent and reliable properties could make the commercialization of PC/MWCNTs composite more promising.

References

1. Singh, S.; Pei, Y.; Miller, R.; Sundararajan, P. R. *Adv Funct Mater* 2003, 13, 868.
2. Sung, Y. T.; Kum, C. K.; Lee, H. S.; Byon, N. S.; Yoon, H. G. *Polymer* 2005, 46, 5656.

3. Satapathy, B. K.; Weidisch, R.; Pötschke, P.; Janke, A. *Macromol Rapid Commun* 2005, 26, 1246.
4. Eitan, A.; Fisher, F. T.; Andrews, R.; Brinson, L. C.; Schadler, L. S. *Compos Sci Technol* 2006, 66, 1162.
5. Fornes, T. D.; Baur, J. W.; Sabba, Y.; Thomas, E. L. *Polymer* 2006, 47, 1704.
6. Sandler, J.; Schffer, M. S. P.; Prasse, T.; Bauhofer, W.; Schulte, K.; Windle, A. *Polymer* 1999, 40, 5967.
7. Andrew, R.; Jacques, D.; Minot, M.; Rantell, T. *Macromol Mater Eng* 2002, 287, 395.
8. Haggenueller, R.; Gommans, H. H.; Rinzler, A. G.; Fischer, J. E.; Winey, K. I. *Chem Phys Lett* 2000, 330, 219.
9. Lozano, K.; Bonilla-Rios, J.; Barrera, E. V. *J Appl Polym Sci* 2002, 80, 1162.
10. Chen, L.; Pang, X. J.; Yu, Z. L. *Mater Sci Eng A* 2007, 457, 287.
11. Satapathy, B. K.; Weidisch, R.; Pötschke, P.; Janke, A. *Compos Sci Technol* 2007, 67, 867.
12. Pötschke, P.; Fornes, T. D.; Paul, D. R. *Polymer* 2002, 43, 3247.
13. Pötschke, P.; Dudkin, S. M.; Alig, I. *Polymer* 2003, 44, 5023.
14. Pötschke, P.; Bhattacharyya, A. R.; Janke, A. *Eur Polym J* 2004, 40, 137.
15. Pötschke, P.; Btünig, H.; Janke, A.; Fischer, D.; Jehnichen, D. *Polymer* 2005, 46, 10355.
16. Pötschke, P.; Kretschmar, B.; Janke, A. *Compos Sci Technol* 2007, 67, 855.